
The Importance of Fibres in Achieving Impact Tolerant Composites

K. M. Prewo

Phil. Trans. R. Soc. Lond. A 1980 **294**, 551-558

doi: 10.1098/rsta.1980.0064

Email alerting service

Receive free email alerts when new articles cite this article - sign up in the box at the top right-hand corner of the article or click [here](#)

To subscribe to *Phil. Trans. R. Soc. Lond. A* go to: <http://rsta.royalsocietypublishing.org/subscriptions>

The importance of fibres in achieving impact tolerant composites

BY K. M. PREWO

United Technologies Research Center, East Hartford, Ct 06108, U.S.A.

[Plate 1]

The damage tolerance and reliability of two different types of fibre reinforced composite materials are described. In both cases it can be shown that properties necessary for reliable engineering application can be achieved by the incorporation of high strength, high modulus brittle fibres in their microstructures. The brittle fibre – ductile matrix system of boron reinforced aluminium is examined first. It is shown that the ability of this system to dissipate impact energy can exceed that of a monolithic unreinforced titanium alloy. This superiority, however, is extremely test dependent and a method of data presentation is used which clearly elucidates the importance of boron fibre diameter. The second system discussed is graphite fibre reinforced glass and it is shown that, despite the fact that both constituents are quite brittle, a tough material is obtained by this combination.

INTRODUCTION

The impact tolerance and reliability of fibre reinforced composites has been, and still remains, a subject area of great concern for those interested in applying these materials to advanced gas turbine engines. This high level of concern stems from the many observations that, under particular applied stress situations, composite materials fail in a brittle manner. Although these observations are indeed valid, it can be shown that under other stress states composite failure need not be classified as brittle and, as will be shown below, it can even be judged to be ‘ductile’.

Two widely differing types of composite materials will be examined in this paper. The first is boron fibre reinforced aluminium, a brittle fibre reinforced ductile matrix system. In contrast, the second system of graphite fibre reinforced glass consists of both brittle fibre and brittle matrix. Although these systems differ widely in character, it will be shown that each can offer resistance to damage.

BORON REINFORCED ALUMINIUM

Boron fibre reinforced aluminium is currently being considered for the fabrication of first stage fan blades for advanced gas turbine engines. In this type of application the material will be subjected to impact by a wide range of foreign objects such as gravel, ice and birds. At present unreinforced titanium alloys are used in this application with great success owing to their high toughness. The much higher elastic stiffness and lower density of boron–aluminium offers significant potential for fan blade improvement. Until recently, however, it appeared that the low levels of composite damage tolerance would limit application to second or third stages of gas turbines which are protected from the incidence of large foreign object impact.

More recently, however, it has been shown that, through the use of large diameter boron fibres, it is possible to achieve very high levels of impact energy dissipation (Prewo 1972, 1976;

[143]

McDanel & Signorelli 1976). A typical example for the experimental verification of this point is shown in figure 1. The photograph is of a standard V-notched Charpy impact specimen of aluminium reinforced with 200 μm diameter boron fibres. The aluminium alloy is of the 1100 type, i.e. 99% pure aluminium, and it can be seen quite clearly that the specimen has undergone extensive plastic deformation during the impact test. This large-scale deformation caused the dissipation of 95 J of energy, which is four times the value obtained from an identically configured titanium alloy (Ti-6%Al-4%V) specimen (see table 1). The reasons for this exceptional composite impact performance are many, and they relate to the properties of the fibre, the strength of the matrix, the quality of the fibre-matrix bond and the test geometry.

TABLE 1. COMPARISON OF IMPACT ENERGY VALUES FOR FULL SIZED NOTCHED CHARPY SPECIMENS CONTAINING 55% BORON FIBRE

fibre diameter/ μm	matrix	total impact energy/J
200	1100 Al	95
145	1100 Al	55
145	6061	35
unreinforced	Ti-6Al-4V	25
unreinforced	6061-T6	15

Of all of these properties, it is the diameter of the fibre and its importance which has received the greatest attention. Boron fibres of 100 μm , 145 μm and 200 μm diameter are all currently available; however, it is only with the largest diameter fibre that the highest levels of impact energy dissipation have been achieved. Because the mechanical properties of boron fibres are substantially independent of fibre diameter, the mechanisms used to describe enhanced composite impact behaviour rely on the pull-out of matrix-coated fibres and the existence of larger areas of matrix between the fibres which can deform extensively. As can be seen from figure 1, however, it is unlikely that any one mechanism can describe all the events that take place during specimen deformation and fracture. The specimen exhibits a great deal of local deformation at the line of contact with the impact striker owing to the very high compression loading. It also exhibits very extensive shear deformation and some local interply delamination near the specimen midplane, which extends for the full length of the specimen causing significant change in the overall specimen shape. Finally, failure at the base of the notch occurred by a combination of interply failure and fibre pull-out; however, the pull-out is of fibres that are coated with aluminium, i.e. extensive shear failure occurred in the matrix surrounding the fibres. The existence and magnitude of all these mechanisms are dependent on the conditions of testing, and thus it cannot be stated that the 200 μm diameter fibre provides a more impact-resistant composite for all cases of impact testing. The following will show how a meaningful comparison of composition performance can be made to elucidate the true role of the fibre in achieving superior impact tolerance.

Impact test

The pendulum impact test is a particularly useful method for examining the performance of various composite materials. Because of the small specimen size and relative ease of testing, it is possible to examine the effects of a wide range of material parameters on impact tolerance. It is a particularly useful method when the impact striker, or tup, is instrumented with strain



FIGURE 1. A fractured V-notched Charpy impact specimen consisting of 200 μm diameter boron fibres reinforcing 1100 (99% Al) aluminium. Note the extensive deformation.

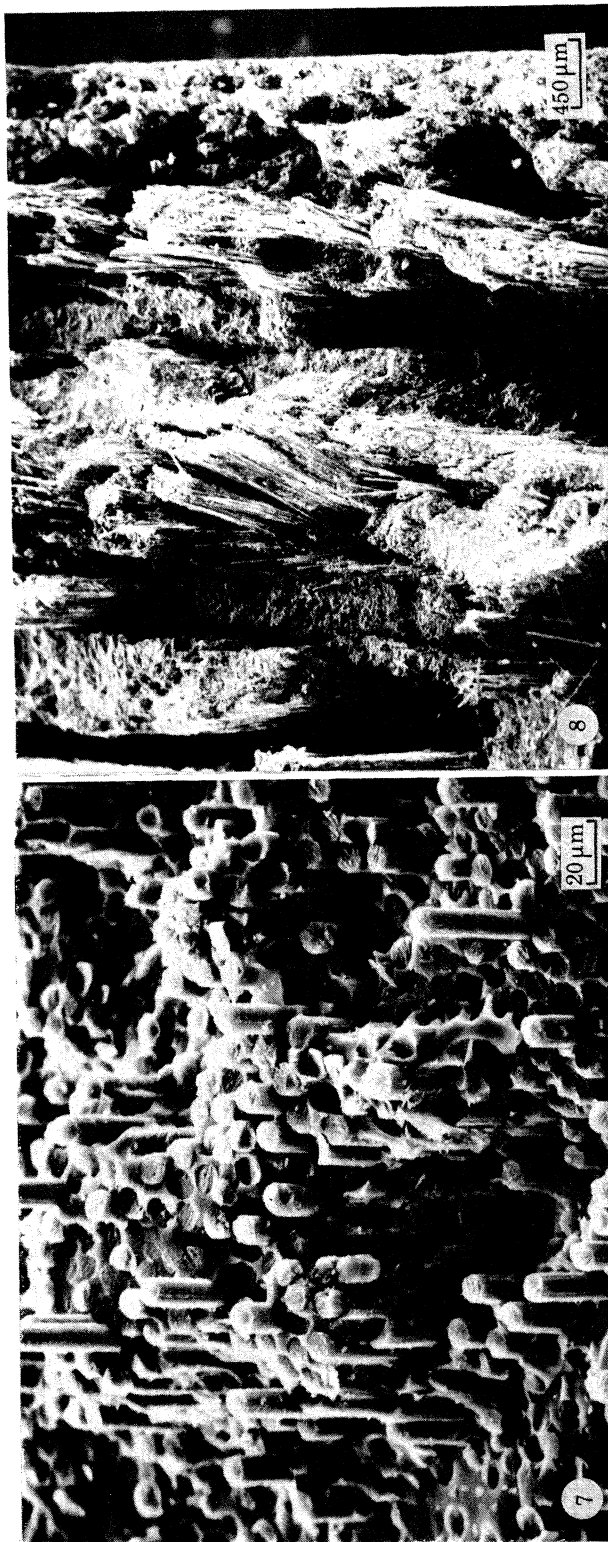


FIGURE 7. The fracture surface of HM graphite fibre reinforced borosilicate glass showing the level of fibre pull-out in locally well bonded regions.

FIGURE 8. Overall fracture surface of HM graphite fibre reinforced borosilicate glass illustrating fracture along fibre bundle boundaries.

gauges so that (after calibration of the strain gauge system) the actual loads applied during the test can be recorded. The data can then be treated in a manner completely analogous to those obtained in a three-point bend test.

Simple equations exist for the prediction of the nominal levels of maximum shear stress and flexural stress generated during the threepoint bend testing of a beam of rectangular cross section. Given a bending span of length L , specimen depth h and width b , the maximum shear stress occurring at the neutral axis can be given by

$$\tau_{\max} = \frac{3}{4}P/bh. \quad (1)$$

The maximum flexural stress occurring at the same time is

$$\sigma_{\max} = \frac{3}{2}(PL/bh^2), \quad (2)$$

and occurs at mid-span on the side away from the loading nose.

The ratio of maximum applied flexural stress to maximum shear stress is given by

$$\sigma_{\max}/\tau_{\max} = 2L/h. \quad (3)$$

Thus, depending on the relative magnitudes of composite material flexural and shear strengths, and the value of span : depth ratio, a specimen can fail in either shear or flexural tension.

The use of these equations presupposes a series of assumptions which are satisfied quite well by composites of the types described in this paper and for which the principal axes of orthotropy coincide with the axes of symmetry of the test specimen. These equations are recognized by the author to be over-simplified in view of the effects of stress concentrations in the areas of the loading points, and more rigorous stress analyses exist for the characterization of the existent stresses, particularly for multiaxially reinforced specimens (Sattar & Kellog 1969; Kedward 1972). However, as will be demonstrated, these simple equations are useful in rationalizing and predicting composite beam response.

Interaction diagram

Experimental verification for the use of the above equations was provided through the three-point bend testing of specimens of 6061 aluminium reinforced with 145 μm diameter boron fibre. The specimens were all unnotched and unidirectionally reinforced, with the fibres oriented parallel to the specimen span L , and tests were run over a wide range of span L : depth h ratios. Three of the measured load against deflexion traces are shown in figure 2. These curves clearly illustrate the importance of applied stress state to the determination of composite material performance, they range from a relatively ductile appearance, $L/h = 4$, to a decidedly brittle fracture, $L/h = 20$. This variation can be explained by noting that the deformation of the composite in the low L/h region is controlled by the shear deformation of the specimen, while at high L/h the much higher flexural stresses that are generated control composite fracture.

Flexural strengths based on maximum load to failure are plotted against L/h in figure 3. As discussed above, the apparent flexural strength is a function of L/h , and only for large values of L/h does the flexural strength reach a constant level. The sloping line for low values of L/h was calculated from the known shear strength of 6061 aluminium and it agrees well with the observed decrease in apparent flexural strength. The actual matrix shear strength was multiplied by a factor of 1.15 which is introduced to include the effects of constraint due to the fibres present. This type of diagrammatic representation is referred to as an 'interaction' diagram (Mullin & Knoell 1970; Christiansen 1974).

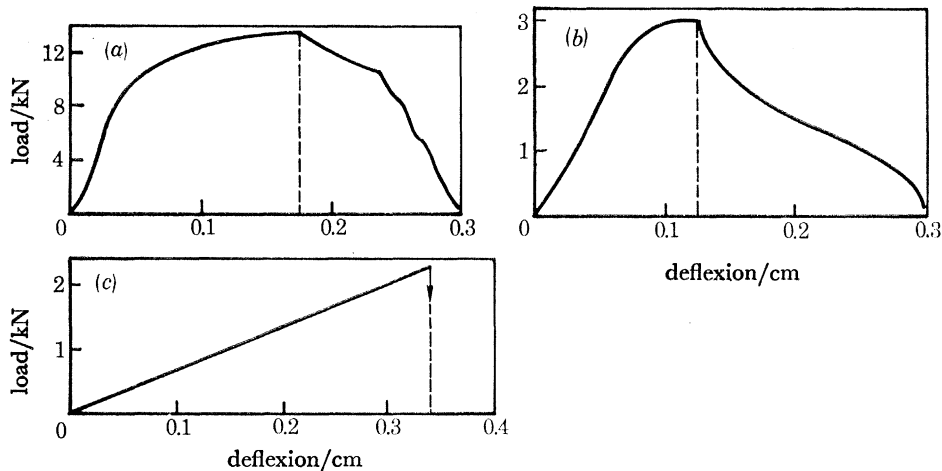


FIGURE 2. Applied load against mid-span deflection for the three point bend testing of unnotched 145 μm diameter boron reinforced 6061 aluminium. Note the change from ductile to brittle appearance with increasing span : depth (L/h) ratio. (a), $L/h = 4$; (b), $L/h = 11$; (c), $L/h = 20$.

Also included in figure 3 are composite flexural strength values obtained by the use of strain gauges placed directly on the tension side of the bend specimens. The gauges were placed at the point of expected maximum tensile stress and gauge output was monitored continuously during specimen three-point bend loading. Composite stress was calculated from the measured

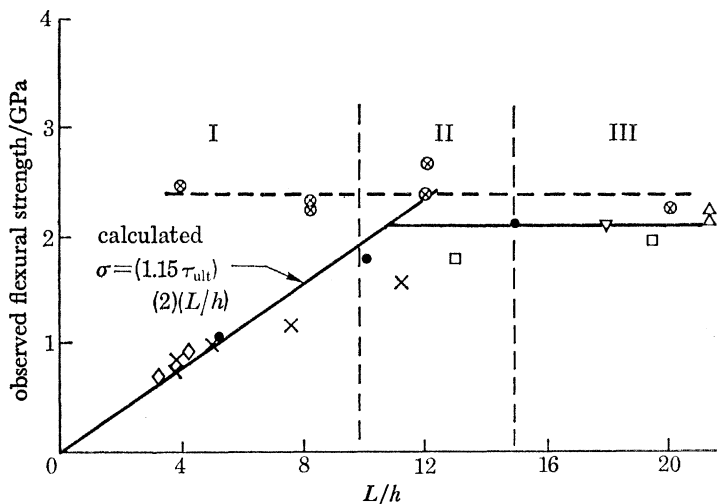


FIGURE 3. Interaction diagram representation of calculated specimen flexural strength as a function of L/h ratio for 145 μm boron reinforced 6061 aluminium. Region I corresponds to rounded load against deflection three point bend curves. Region II corresponds to partially rounded curves and region III corresponds to completely linear curves. The \odot data points were obtained by using strain gauge readings while the other data points were obtained for various lengths of span, L .

failure strain values for the outer plies and composite elastic modulus. The calculated values of strength were essentially independent of L/h and agreed well with those obtained from the simple beam analysis in the high L/h region. This is as it should be since the tensile strength of the outer ply should be independent of specimen geometry and only for high L/h values is agreement with the beam calculation expected.

Effect of fibre diameter on interaction diagram

With this interaction diagram formulation, a wide range of 145 μm diameter and 200 μm diameter boron fibre reinforced 1100 aluminium specimens were tested in three-point bend and instrumented impact. Both notched and unnotched specimens were tested and it was found that, if the value of h is chosen in the stress calculation to equal the remaining unnotched specimen thickness, the presence of the notch had no measurable effect on specimen bend strength. All of the data obtained can be described by a single interaction diagram curve (figure 4) for fibres of both diameters. This is to be expected since neither the matrix shear strength (controlling low L/h region) nor the composite flexural strength (controlling the high L/h region) are dependent on fibre diameter.

Data are also presented in figure 4 for unreinforced titanium alloy (Ti-6Al-4V) and aluminium alloy (6061-T6) which were tested by pendulum three-point bend impact of V-notched specimens. The value of L/h was varied by changing both the notch depth and also the overall

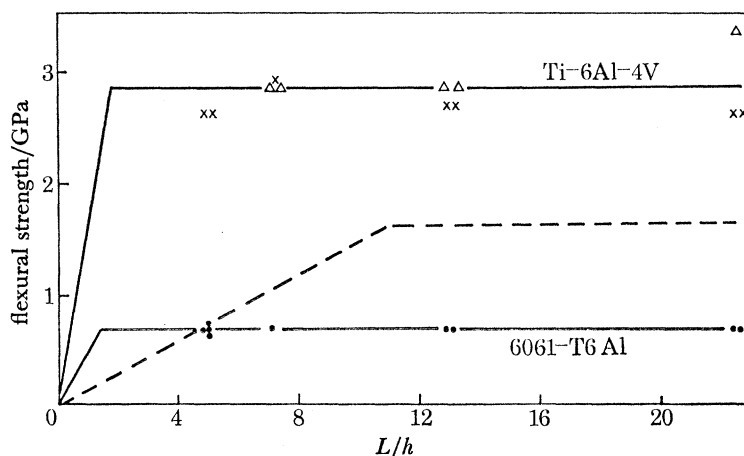


FIGURE 4. Interaction diagram comparison of 200 μm diameter and 140 μm diameter boron reinforced 1100 aluminium (---) with titanium (Ti-6Al-4V) and aluminium (6061-T6) alloys.

specimen thickness. It is interesting to note the constant level of flexural strength obtained. No data were obtained in the very low L/h region (where a fall in strength might be expected) as a result of specimen size restrictions. Therefore, the extensions of the drawn curves into this region are conjecture and were calculated for the sake of completeness. The values of observed flexural strength for these materials were found to be quite high and correspond to between 2.5 and 2.9 times the tensile yield strengths of the alloys. This is reasonable in the presence of the notch constraint.

Composite impact energy

The interaction diagram presents only a partial picture of material performance. It is capable of describing the load-carrying ability of the composite but not the energy dissipation capability. Owing to the large variation in the shapes of the curves shown in figure 2, it is to be expected that the ability to dissipate energy would vary greatly with specimen geometry. This can be illustrated by taking the energy required to raise a specimen to the maximum load prior to failure. In figure 2 this corresponds to the area under each of the curves between the beginning

of the test up to the dotted vertical line. When this energy is divided by the volume of the specimen under stress, a very strong dependence on L/h is evident (figure 5). In the high L/h region (flexural strength controlled), this value reaches the theoretical limit calculated for fully elastic behaviour, as shown in the figure for the 145 μm diameter boron reinforced 6061.

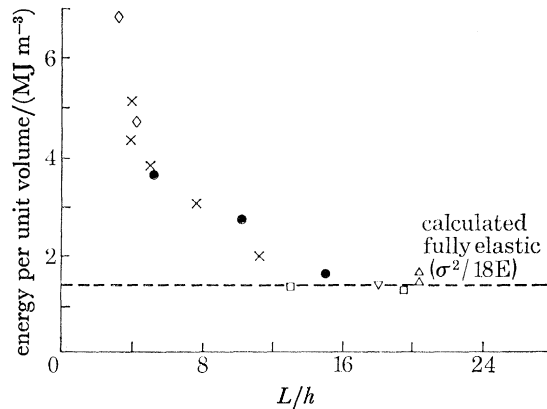


FIGURE 5. The energy per unit volume of test specimen required to raise an unnotched three-point bend specimen to the maximum applied load. The material is 145 μm boron reinforced 6061 aluminium and the different data point shapes refer to varying span lengths.

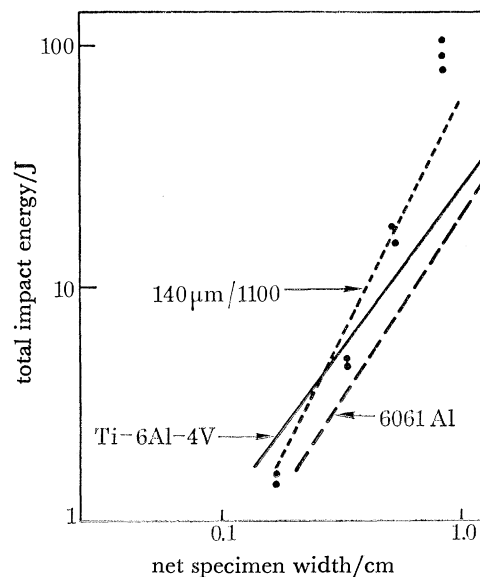


FIGURE 6. The total energy required to fracture impact specimens in a three-point bend configuration. The boron/aluminium data are for both notched and unnotched specimens while the titanium and aluminium alloy data were obtained with notched specimens only. ●, 200 $\mu\text{m}/1100$.

In impact damage situations it may be the total energy to fracture that is most important rather than just the energy absorbed to the point of instability. It is this total value of energy which has been shown to be greatest for 200 μm diameter fibre reinforced composites and corresponds to the total area under the load/deflexion trace. Once again, it can be shown that this property varies with test geometry and can be compared with the performance of unreinforced monolithic metals. The form of representation is based on a technique used to describe

the toughness of notched metals and is a log-log plot of total impact energy dissipated against the net specimen section, h , beneath the notch. The data are presented in figure 6 comparing 140 μm and 200 μm diameter boron reinforced 1100 aluminium with 6061 and Ti-6Al-4V. The data for the 140 μm fibre reinforced 1100 are for both notched and unnotched specimens, while all the other data in the figure are for notched specimens. It can be seen, however, that the larger diameter fibre composite does, indeed, dissipate considerably more energy only in the thick specimen (large h). At smaller h values (larger values of L/h for constant L) the elastic behaviour of the material becomes more important and the difference between the two types of fibre reinforced material disappears. It is interesting to note that a superiority of boron/aluminium over Ti-6Al-4V also disappears at small values of h .

Thus, by using both the interaction diagram (figure 4) and the total energy diagram (figure 6) to represent the pendulum impact performance of composites it is possible to elucidate the effects of fibre diameter. It appears that under those impact conditions where shear stresses are high, the larger fibres induce more extensive plastic deformation of the composite matrix and hence dissipate more energy. In the case of fracture primarily due to high tensile stresses, the fibre diameter is of little or no importance.

GLASS MATRIX COMPOSITES

The previous section has illustrated the case of ductile matrix-brittle fibre reinforced composites where the intention is to maintain the impact damage tolerance and toughness of the monolithic material despite the addition of brittle fibres. In this second section, however, the approach is quite different in that one starts with a brittle glass matrix and attempts to impart an increased degree of toughness by the addition of brittle fibres. This has been illustrated in the past (Phillips *et al.* 1972; Phillips 1974) and is extended here for the case of graphite fibre reinforced glass matrix composites.

TABLE 2. FRACTURE TOUGHNESS OF HM FIBRE REINFORCED BOROSILICATE
GLASS MATRIX COMPOSITES

test temperature/ $^{\circ}\text{C}$	test speed/(cm s^{-1})	fracture toughness, $K_{\text{c}}/\text{MPa m}^{\frac{1}{2}}$
22	330.0	21.4
22	0.002	22.4
600	330.0	15.8
650	330.0	19.0

In this case the test technique chosen is analogous to that used in the determination of the fracture toughness of monolithic materials. Pre-notched composite specimens were tested in three-point bend and the fracture toughness values calculated were based on the maximum load achieved prior to fracture. The material tested was HMS graphite fibre reinforced borosilicate glass fabricated as part of a continuing programme (Prewo & Bacon 1978) to develop this composite system for structural use. A summary of the fracture toughness data obtained for this system is given in table 2. The data demonstrate that, despite significant variations in test temperature and test speed, the level of fracture toughness measured is quite high. These data compare favourably with values typical of graphite fibre reinforced epoxy resins and unreinforced metals, and demonstrate that the fracture toughness of this composite system can

reach levels necessary for engineering application. The ability to withstand a very high level of stress in the presence of a notch can be related to the low strength of the matrix and its inability to maintain high levels of stress near a graphite fibre. Thus the stress concentration effect is substantially obviated and the initiation of large-scale crack growth is difficult. The further extension of the crack is also very difficult because of the many energy dissipation mechanisms that operate. These include the behaviour of individual fibres and also the fracture of bundles of fibres. This latter mechanism operates because the microstructure of the composite is not completely homogeneous, each of the graphite fibre tows being separated from its neighbours by a glass-rich area which provides a path for crack diversion. Both individual fibre fracture and pull-out, and fibre bundle fracture and pull-out occur (figures 7 and 8).

CONCLUDING REMARKS

Although advanced fibre reinforced composites achieve their high strength and stiffness levels through the presence of significant percentages of brittle fibres, the resultant composites need not be considered brittle. Complex failure modes, which rely on the inhomogeneity of the composite microstructure, can provide high levels of material toughness and impact tolerance. The extent to which these mechanisms operate relates strongly to the characteristics of the composite reinforcing fibres, and the nature of these fibre properties has been the subject of considerable research during recent years. As in the case of monolithic materials, however, the performance of the composite is a direct consequence of the applied stress state and its interaction with the available material deformation modes. Thus, the importance of fibre properties, or any other material variables for that matter, must be assessed in light of the imposed stress state.

REFERENCES (Prewo)

- Christiansen, A. W. 1974 *Fibre Sci. Technol.* **7**, 1.
 Kedward, K. T. 1972 *Fibre Sci. Technol.* **5**, 85.
 McDanel, D. L. & Signorelli, R. A. 1976 *Failure modes in composites III*, New York: The Metallurgical Society of A.I.M.E.
 Mullen, J. V. & Knoell, A. C. 1970 *Mater. Res. Stand.* **10**, 16.
 Phillips, D. C. 1974 *J. Mater. Sci.* **9**, 1847–1854.
 Phillips, D. C., Sambell, R. A. J. & Bowen, D. H. 1972 *J. Mater. Sci.* **7**, 1454–1464.
 Prewo, K. M. 1972 *J. Compos. Mater.* **6**, 442.
 Prewo, K. M. 1976 *Failure modes in composites III*. New York: The Metallurgical Society of A.I.M.E.
 Prewo, K. M. & Bacon, J. F. 1978 *Proceedings of Second International Conference on Composite Materials*. New York: The Metallurgical Society of A.I.M.E.
 Sattar, S. A. & Kellog, D. H. 1969 *ASTM-STP-460*, p. 62.

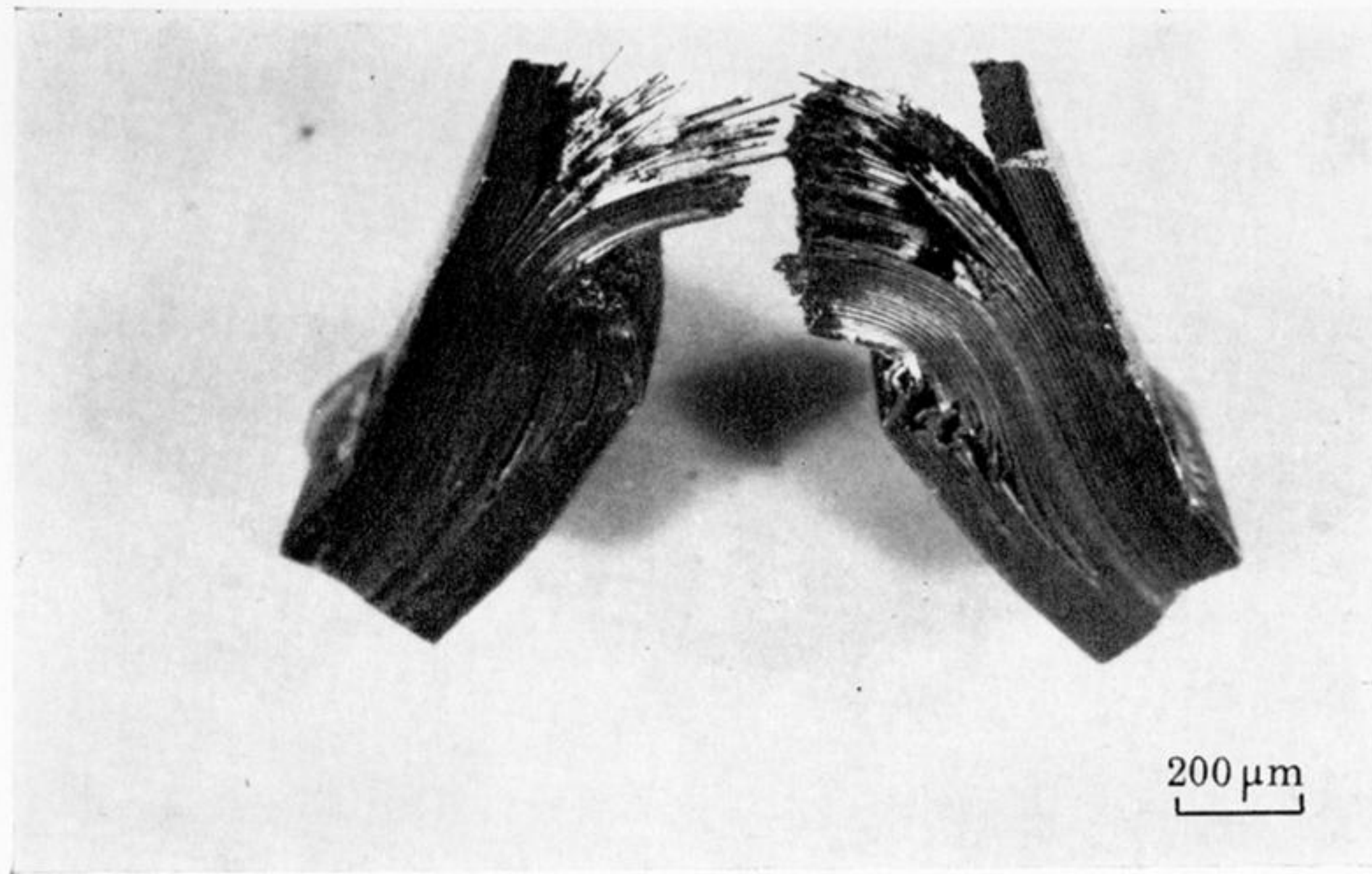


FIGURE 1. A fractured V-notched Charpy impact specimen consisting of 200 μm diameter boron fibres reinforcing 1100 (99 % Al) aluminium. Note the extensive deformation.

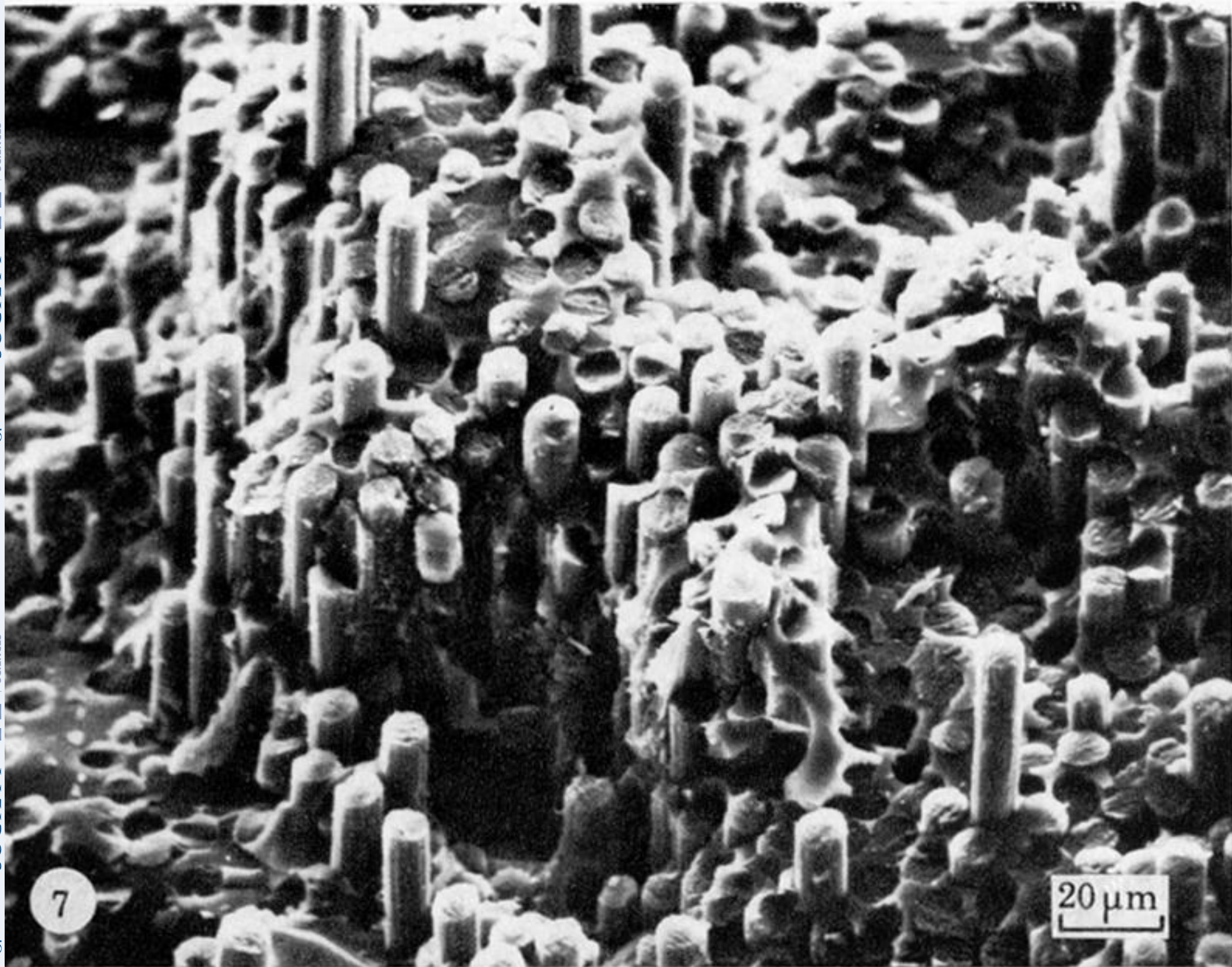


FIGURE 7. The fracture surface of HM graphite fibre reinforced borosilicate glass showing the level of fibre pull-out in locally well bonded regions.

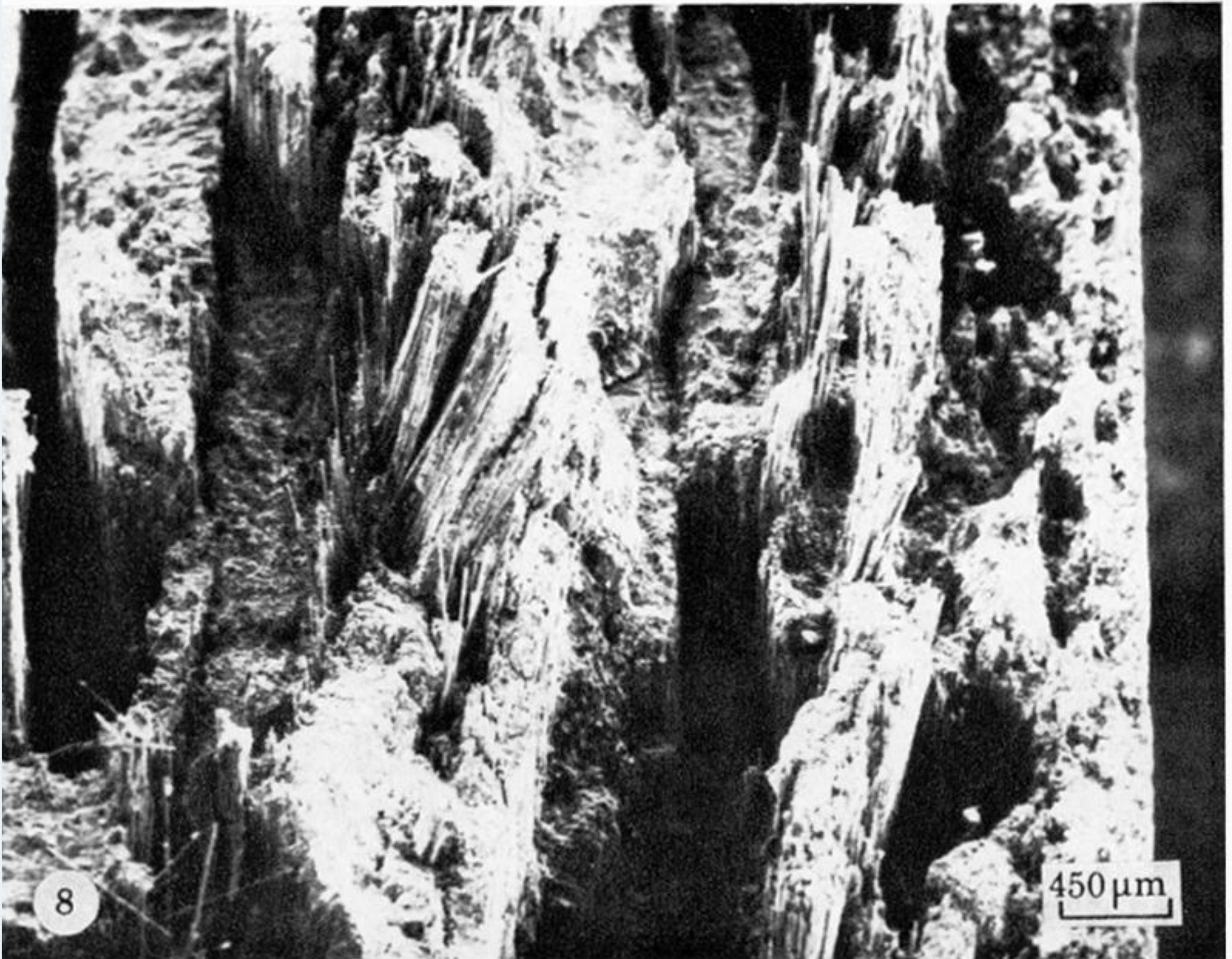


FIGURE 8. Overall fracture surface of HM graphite fibre reinforced borosilicate glass illustrating fracture along fibre bundle boundaries.